



## UvA-DARE (Digital Academic Repository)

### Coherent X-ray scattering of charge order dynamics and phase separation in titanates

Shi, B.

**Publication date**

2017

**Document Version**

Other version

**License**

Other

[Link to publication](#)

**Citation for published version (APA):**

Shi, B. (2017). *Coherent X-ray scattering of charge order dynamics and phase separation in titanates*. [Thesis, fully internal, Universiteit van Amsterdam].

**General rights**

It is not permitted to download or to forward/distribute the text or part of it without the consent of the author(s) and/or copyright holder(s), other than for strictly personal, individual use, unless the work is under an open content license (like Creative Commons).

**Disclaimer/Complaints regulations**

If you believe that digital publication of certain material infringes any of your rights or (privacy) interests, please let the Library know, stating your reasons. In case of a legitimate complaint, the Library will make the material inaccessible and/or remove it from the website. Please Ask the Library: <https://uba.uva.nl/en/contact>, or a letter to: Library of the University of Amsterdam, Secretariat, Singel 425, 1012 WP Amsterdam, The Netherlands. You will be contacted as soon as possible.

# Appendix B

## The Timepix Detector

The Timepix detector [135–137, 109, 138, 123] is a derivative product of the Medipix detector developed for high energy particle detection at CERN. In this detector, the signal from each pixel is processed by its own electronic circuit, which differs from the operating principle of conventional CCD detectors. This simultaneous readout ability allows one to record up to 120 frames per second, making it a suitable detector for the 120 Hz repetition rate of the LCLS.

As we were only the second user group to utilize this detector, and since we could benefit from direct contact with the manufacture of the instrument at Amsterdam Scientific Instruments, we will describe it in some detail here. In particular, we discuss the sensitivity of the detector, the use of cluster analysis to detect pixels that have received multiple photons in a single shot, and the effects of charge sharing.

Fig. B.1 shows a typical Timepix chip. It consists of a 300  $\mu\text{m}$  thick silicon diode on the top, which is bridged by 30  $\mu\text{m}$  In-Sn bump-bond balls to an application-specific integrated circuit (ASIC)[137, 109].

As in any diode, photons hitting the detector produce a number of electron-hole excitations that is proportional to the photon energy. The electrons and holes drift apart under the influence of a 100 V bias voltage (see Fig. B.2). The holes are collected by contacts at the back side of the wafer and then processed on the ASIC chip. The metallic contacts form a matrix of 256x256, dividing the photodiode in 55x55  $\mu\text{m}^2$  pixels. Four of such quadrants are connected by two rows of 165  $\mu\text{m}$  by 55  $\mu\text{m}$  rectangular pixels, that form a cross at the center of the detector (see Fig. 4.10(b) for an example in which the borders of the quadrant are visible).

The electronics can process the signal in 3 different modes depending on the user setting: the counting mode, the Timepix mode, and the time-over-threshold (ToT) mode. In the experiments described here, the detector was operated in the ToT mode. In this mode the

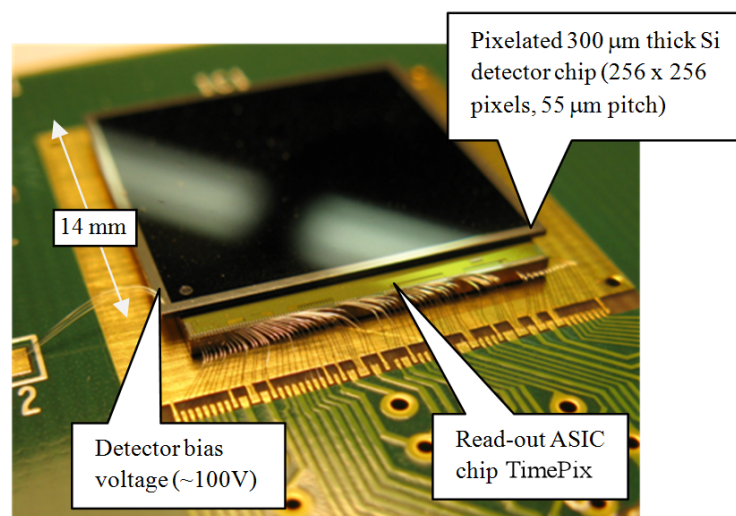


Fig. B.1 Picture of the Timepix detector. An application-specific integrated circuit (ASIC) is attached to the silicon sensor with Indium bump-bonding. Adopted from the Timepix website.

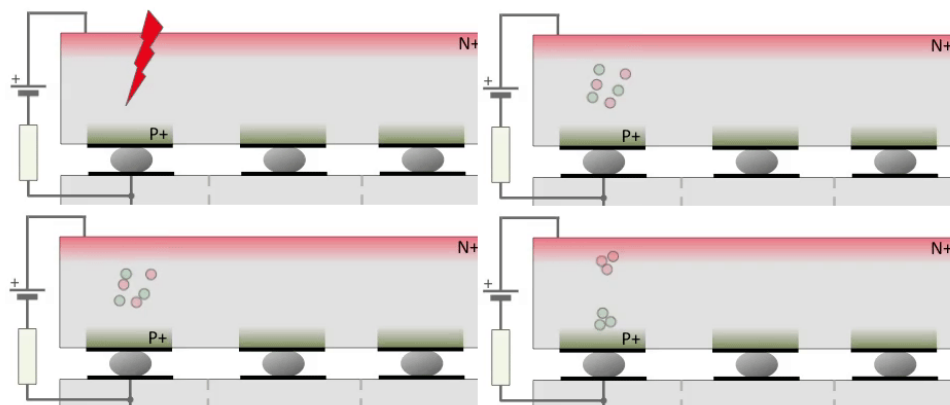


Fig. B.2 Schematic of the Timepix detector showing the pixelated p-n diode sensor that is bump bonded to the underlying signal processing unit, and an animation of the photon detection on the top layer. From the top-left to the bottom-right, the process is as follows: photons hit the top silicon layer creating electron-hole pairs. A bias voltage of around 100 V causes the holes move to the readout, while the electrons move towards the surface. The number of electron-hole pairs is proportional to the incident photon energy. Adopted from Timepix website.

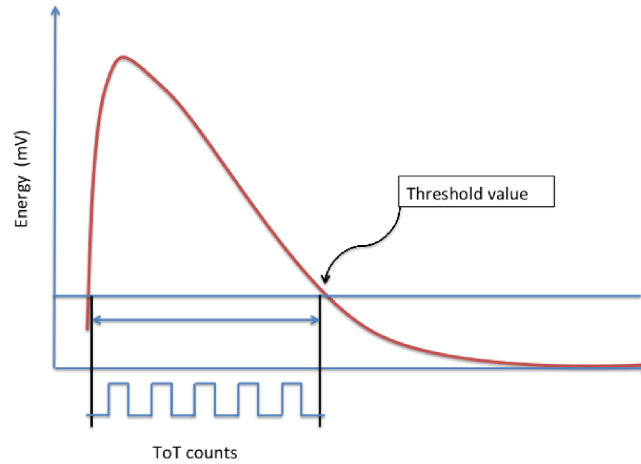


Fig. B.3 The counting logic of the ToT mode. The pre-amplifier converts the collected charges into a standard pulse shape, whose integral is proportional to this charge and accordingly proportional to the photon energy. The signal is the number of cycles of a 40 MHz internal clock that are counted while the input pulse is over the preset threshold voltage.

charge pulse generated by the incident photons is converted to a standard shape voltage pulse whose integral is proportional to the collected charges. This pulse is compared to a discriminator level (see Fig. B.3) that is set such that the electronic noise in the detection circuit is suppressed. The output is given by the number of 40 MHz clock pulses for which the signal is above the threshold. The advantage of this operation mode is that it yields the most precise estimate of the charges that collected by the pixel and thus the deposited photon energy. However, this ToT circuitry has a non-linear response at photon energies below 18 keV [139]. For instance, if the amount of charge is insufficient to bring the signal above the discriminator level, it will be lost completely.

The calibration curve that relates the amount of charge (= energy of the photon) to the ToT output is shown Fig. B.4 [140]. Assuming a Gaussian photon energy distribution, the corresponding ToT output will be distorted by the non-linear response function, resulting a distorted Gaussian output distribution.

The response curve is well described by the fitting function

$$S_{ToT}(E) = aE + b - \frac{c}{(E - t)}, \quad (\text{B.1})$$

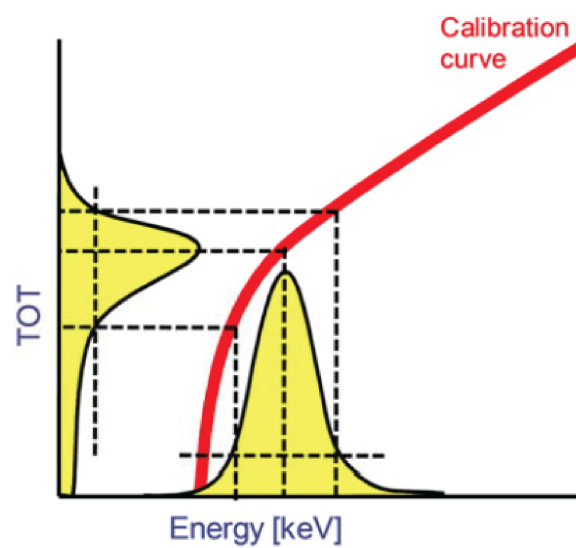


Fig. B.4 The relation between photon energy and ToT response. The red curve represents the calibration curve. The horizontal yellow Gaussian area represents the energy distribution of the photons hitting the detector. The vertical yellow area represents the resulting ToT signal distribution. At low energy, the ToT probability function can be fitted with a distorted Gaussian; at high energy the ToT response is close to linear with photon energy. Adopted from [140].

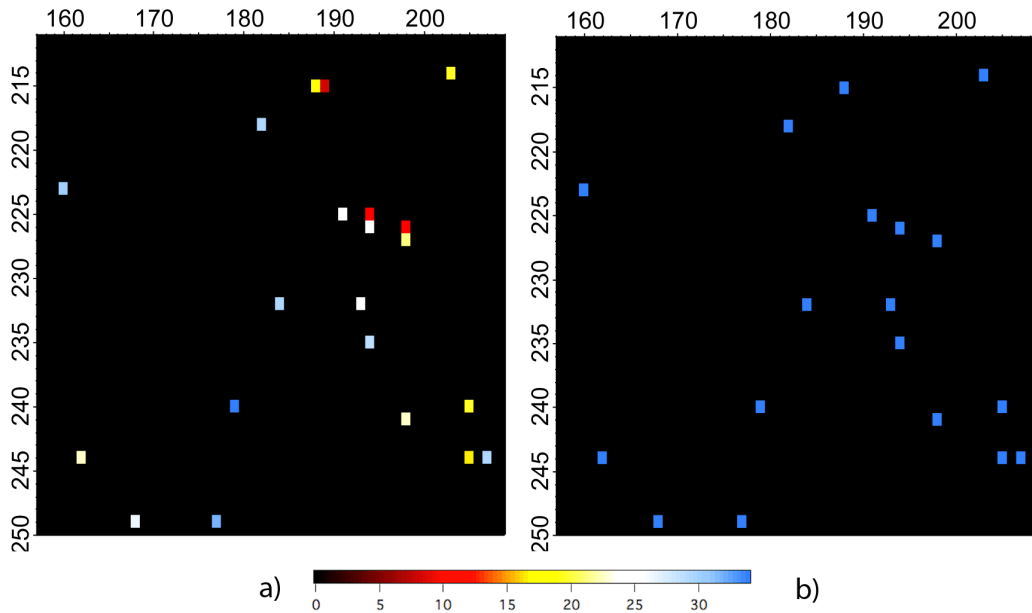


Fig. B.5 a) A portion of raw data of the (022) diffracted beam intensity of a single LCLS pulse. The colored dots represent the illuminated pixels, and the black background represents zero counts. Most events are single pixel events, but one can also observe 2 pixel clusters in the shown region. b) After cluster analysis and correction for charge sharing, the counts of the multipixel clusters have been reassigned to single pixel photon events.

where  $S_{ToT}$  is the ToT number of clock pulses,  $E$  is the photon energy,  $a, b, c$  and  $t$  are fitting parameters. These can be determined by fitting to data of radiation sources with well defined energy.

## B.1 Charge sharing

An intrinsic problem of pixelated detectors is the charge sharing effect. The charge cloud generated in the detector by an incident photon can spread out on its way to the collector due to Coulomb repulsion and dispersion. This gives rise to charge sharing between pixels. As a result, two or even more pixels each record a fraction of the total charge and it becomes difficult to determine if and where the photon has hit.

To illustrate this, Fig. B.5, left, shows a region of a typical Timepix pattern of the (022) reflection from a single XFEL shot (for experimental settings, please see chapter 4). There are only a few illuminated pixels in the field of view, mainly isolated from each other. However some adjacent pixels are connected into clusters. In these clusters it is not a priori clear whether multiple photons have impinged on the corner of adjacent pixels or that the spatially

separated charges originating from one or more photons have hit over several neighboring pixels.

The situation can be cleared up partially by using a droplet analysis protocol [99], where the counts of the pixels within a cluster are regrouped and assigned to a best guess of the photon impact position. In this procedure, first the total ToT signal of the cluster is divided by the signal of a single photon, which was estimated to be  $\text{ToT}=34$  by calculating the histogram of multiple single frames, such as shown in Fig. B.5. The resulting value is rounded to the nearest integer, giving an estimate of the total number  $n$  of photons in the cluster. Then the pixels in the cluster are sorted from largest to smallest ToT values and the  $n$  photons are assigned to those pixels having the highest values. The result is an image with integer photon counts 0, 1, 2, 3, etc. in each pixel, as shown in the right panel of Fig. B.5.

## B.2 Cluster analysis

Before the droplet analysis can be performed, first all multipixel clusters have to be found. To this end the SoPhy package was developed by J. Uher [123] at Amsterdam Scientific Instruments. This code scans each image for the first non-zero value pixel, giving it a label 1. It then checks the surrounding pixels, and gives non-zero valued pixels the same label. For this first cluster, the positions of pixels in the cluster and their intensity (ToT) are stored. The procedure is iterated until all the detector pixels are evaluated and labeled.

We will illustrate the procedure on a data set consisting of 131,751 Timepix frames exposed by the (022) reflection from single X-ray laser pulses with an energy of 8.08 keV. We used SoPhy to identify the clusters of different sizes, together with their total ToT value for all frames in the movie. In Fig. B.6 (b), we show the accumulated histograms for each cluster size. For single pixel clusters, a single photon peak is resolved. Multi-pixel clusters show histograms with correspondingly larger number of peaks, although they become less clearly resolved beyond 3-4 pixel cluster size.

It is interesting to note that the single photon peak for two pixel clusters is shifted to higher ToT values compared to the single photon peak in the single pixel cluster (see Fig. B.6 (a)). This is due to the fact that in two or more pixel clusters less charge is lost due to charge sharing. The same effect can be seen also in the curves of even bigger cluster sizes.

A comparison between the raw data histogram and the sum of all the cluster histograms is shown in Fig. B.6 (b). This graph makes it clear that by cluster analysis alone, we can resolve peaks corresponding to the detection of up to four photons, the vast majority of which is produced by equal sized clusters though. This result indicates that we don't have multiple photons hitting the same pixel in experiments involving a single LCLS pulse. This is mostly

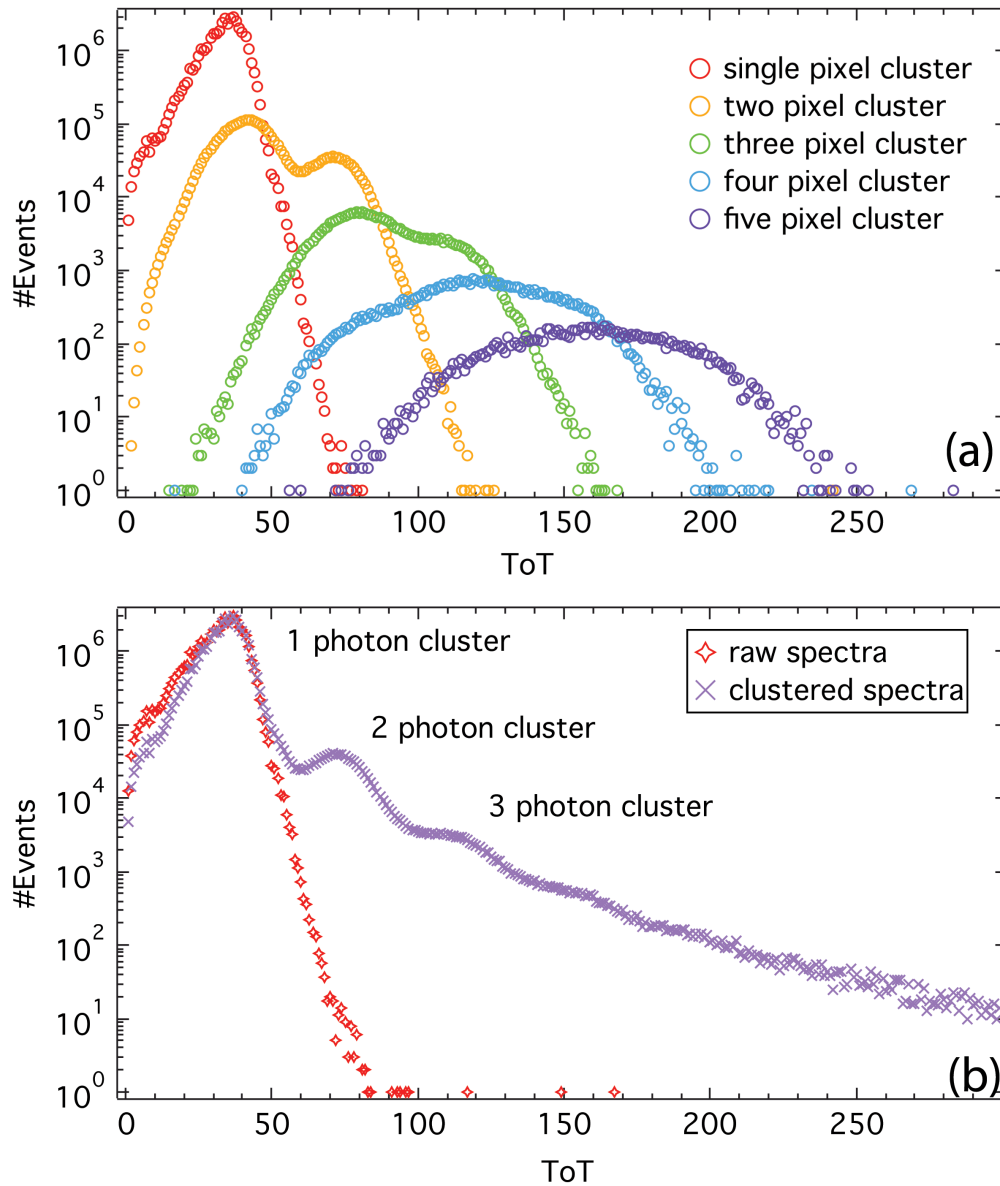


Fig. B.6 (a) Cumulative histograms of the ToT value for each cluster size. The red peak shows the single pixel cluster histogram, which only trivially has a single peak. This indicates that with the incident intensity most commonly used for the experiments reported in chapter 4, the vast majority of single pixel clusters are indeed single photon events. The orange curve shows the histogram of two pixel clusters, in which we can recognize the one and two photon peaks. (b) Raw and clustered Timepix ToT histogram. The red curve is the accumulated raw histogram of the ToT value for 14000 single-shot frames. It shows a single photon peak at  $\text{ToT} = 34$ . The purple curve is the cluster-analyzed histogram, where the events lost due to charge sharing have been recovered. On the purple spectrum, we can clearly identify peaks at multiples of the ToT value of the single photon peak.

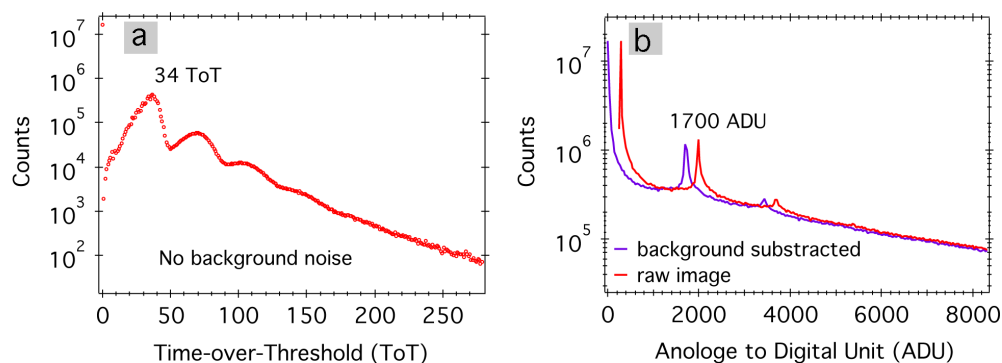


Fig. B.7 Comparison of the Timepix histogram for the 100 shot images shown in Fig.4.12. Discrete photon peaks are visible up to 3 photon events.

due to the attenuation of the incoming beam and the relatively low diffraction efficiency of the sample (more details are given in chapter 4).

To illustrate this, in Fig. B.7 we compare the histograms of the intensities of Timepix and Pixis 1300 images given in Fig. 4.12, which were both illuminated by 100 LCLS shots, but for the Timepix data, the incoming beam was attenuated by a factor 80. The raw Timepix histogram only contains a single photon peak (the red curve in Fig. B.6 (b)). After cluster analysis of 100 single shot Timepix frames, multi-photon events can be seen in the clustered histogram (the purple curve in Fig. B.6 (b)). These multi-photon peaks are very broad, and have a spacing of 34 ToT units. Additionally, the non-linear response curve of the Timepix camera in ToT mode (see Fig. B.4 and related discussions.) deforms shape of the single photon peak in the interval  $0 \sim 50$  ToT counts.

The histogram from the Pixis camera on the other hand shows sharp true multi-photon peaks, corresponding to multiple photons having hit the same pixel during a single 30 fs exposure. The spacing between the peaks is 1700 analogue-to-digital units (ADU) corresponding to one photon.

This part of the appendix shows that although the Timepix detector was the only device enabling fast recording of data at the 120 Hz rate matching the rep-rate of the LCLS, at the time of our measurements, this does come at a price in terms of the need for a detailed analysis of the response of the Timepix system. The analysis presented here, therefore, is of importance for other users of the Timepix at the LCLS in the future.